Advantages of Dual Magnet Ribbon Beam Architecture for Particle Control in Single Wafer High Current Implant

C. Campbell, G. Redinbo, J. Blake, P. Kellerman, E. Moore and N. Variam

Varian Semiconductor Equipment Associates, Inc., 35 Dory Road, Gloucester, MA 01930, USA

Abstract. The issue of particle contamination in ion implant has received renewed interest recently due to the confirmation of killer ballistic particles in batch-style high current implanters. Single wafer high current is now the preferred method of high current implant and device limited yield is now being driven by particles that mask the implant and kill devices. Managing particles will become even more critical to device yields as devices continue to scale to tighter line widths and overall die sizes increase. Just as the batch-style implanters were found to limit yield at smaller device dimensions, the specifics of single wafer implant architectures can affect particle performance. Here we demonstrate the particle performance capability of the Varian VIISta HC dual magnet ribbon beam architecture, analyze the sources of particles in the system and offer an explanation of the physical mechanism that enables on-wafer particle performance.

Keywords: High current implanter, single wafer, particle.

INTRODUCTION

Single wafer high current implant has been adopted as the implant platform of choice for advanced device manufacturing because of the limitations of batch system ballistic particle damage and resulting yield loss [1]. The impact of particle density on device limited yield has been widely understood for some time. In single wafer high current implant the device limited yield is now being driven by the "masking" particles that block the implant and act as the new killer defect. The minimum size of these killer defects has decreased as devices feature sizes have continued to scale. The simultaneous increase of die size has put significant pressure on advanced device manufacturers who need to complete a larger number of high current implant steps while still maintaining acceptable yield. The smaller particles that now limit yield are harder to remove in typical post-implant cleaning steps. This has led to extremely tight particle performance requirements for single wafer high current implant. It is preferable to keep the particles off the wafer than to try to clean them off later.

While implant itself is generally acknowledged to be one of the cleaner processes in the fab, high current implant brings special challenges. The higher currents, power densities, photo-resist out gassing and beam strike make the high current system design requirements more rigorous, both in terms of mechanical wafer handling and beamline design. Between these two major particle sources, mechanical adders can usually be managed through simplified end-station design, reduced mechanical contact and forces, vacuum sequencing and other best practice wafer handling approaches. In terms of beam-borne particles, remedial steps can be taken to reduce sources of beamline particles in the implanter (materials selection, process residue reduction, optics beamstrike, etc) but once these steps are implemented it is clearly best to prevent any particles from being transported to the wafer once they are generated.

It has been established that particles are subject to electrostatic forces in the ion beam itself which can trap and transport the charged particles around an analysis magnet, down the beamline and onto the wafer surface [2]. In this paper we demonstrate the particle performance capability of the dual magnet ribbon beam architecture of VIISta HC, analyze the sources of particles in the system and offer an explanation of the physical mechanism that enables on-wafer performance.

SYSTEM DESCRIPTION

The VIISta HC system is shown in Figure 1 is based on a dual magnet ribbon beam architecture where the first magnet serves to analyze the beam and the second magnet makes the beam uniform and parallel prior to

the wafer. The end-station is comprised of a simple one-dimensional wafer scan that moves the wafer vertically through the parallel ribbon beam at low velocity and acceleration.

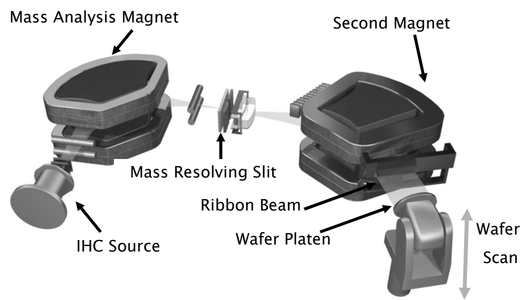

FIGURE 1. VIISta HC dual magnet ribbon beam architecture single wafer high current implanter.

PARTICLE PERFORMANCE

Typical particle performance of VIISta high current systems is shown in Figure 2 where beam borne adders in a logic production process flow are shown. The monitor recipe is a mid-range energy (< 15keV) and high dose (> 1E15 cm^{-2}) with cumulative particles > 0.1µm.

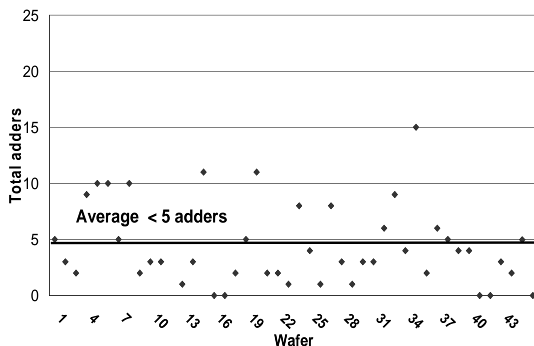

FIGURE 2. Particle adders on a VIISta high current system in logic production. Particle size ≥0.1um over approximately 6 weeks of data collection..

Beam line cleanliness is one critical element of particle performance in high current implanters. Figure 3 shows the inside beam-guide of the mass analyzer and the second magnet of a VIISta HC system that had been run through various recipes for > 700 hours. As is typical in high current beam line implanters, the beam guide of the analysis magnet (Figure 3a) shows evidence of flaking and debris. The mass analysis function of the analyzer magnet results in mass filtering and ion beam strike on beam guide surfaces, which form surface coating, flaking and surface sputtered particulate. In contrast, the inside of the VIISta HC second magnet (Figure 3b) does not show evidence of flaking or particulate, due to the ion beam properties, the magnet properties and the beam-guide design features within the second magnet of VIISta HC. The relative cleanliness of this second magnet beam guide just prior to the wafer, may partially explain the on-wafer particle results achieved in this architecture.

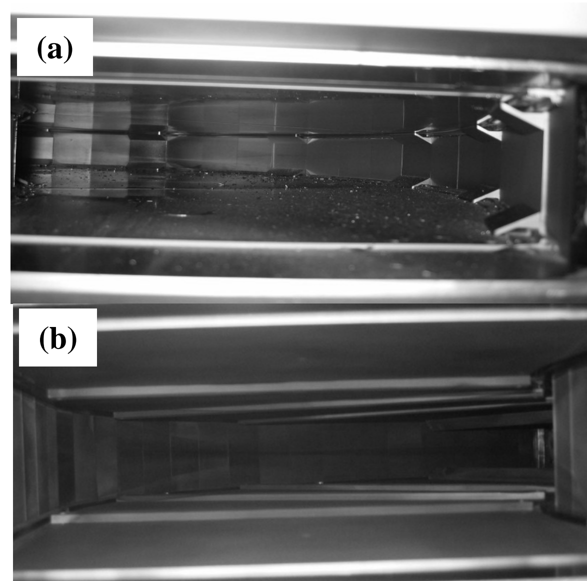

FIGURE 3. Photographs of inside of mass analysis magnet (a) and beam precision magnet (b) after ~ 700 hours of implanter operation.

EXPERIMENT

In order to further investigate the source of particle performance of the VIISta HC system, particle measurements were taken at the entrance of the second magnet with a special wafer edge grip holding fixture. Comparison particle measurements were also taken from wafers in the end-station, after the second magnet sampled with a wafer on the platen. Particle control base-line measurements were collected during a controlled no-beam rough/vent sequence to accurately partition the particle adders to the mechanical transport and rough vent sequence. Beam transport particle measurements were collected both at the wafer plane with a P+ 20keV, 10mA ion beam normally tuned with

a wafer positioned at the entrance of the second magnet as in Figure 4b. Specifically, wafer exposure time was recorded and the wafer was re-positioning to the implant position as shown in Figure 4a. The wafer was implanted with the recorded exposure time with the same beam implant conditions, equivalent to a 5E14 atoms/cm^2 dose. Comparison particle measurements were taken with steady-state ion beam conditions and with induced particle excursion scenarios in the extraction and analyzer magnet regions. Generated particle excursions were induced from analyzer beam guide hammer impacts and intentional mass resolving slit (MRS) beam strike.

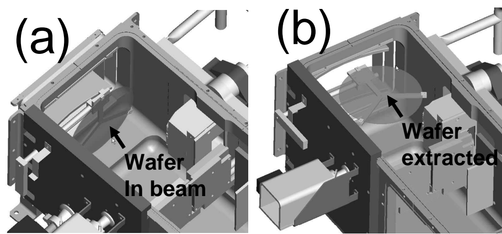

FIGURE 4. Experimental fixture for holding a particle wafer between the magnets. Figure 4a shows a wafer in the ion beam and Figure 4b shows the wafer extracted.

RESULTS

Pre and post-second magnet results from the steady-state P+ 20keV, 10mA, 5E14 atoms/cm^2 implant are shown in Figure 5. Wafer particle measurements taken with KLA-Tencor Surfscan SP1 TBI. Measurements indicate that the pre-second magnet particles are a factor of 6 times higher than the post-second magnet measurements for the .09 - .5μm particles with larger pre vs. post magnet particle reduction factors for the >.5u particle sizes.

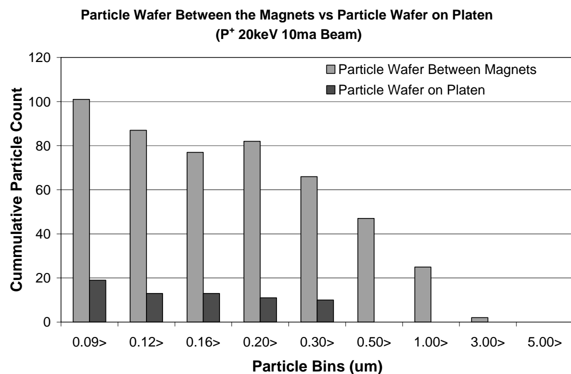

FIGURE 5. On-wafer particle data comparing a wafer placed between the magnets vs a wafer on the platen.

Experimental measurements taken with induced particle excursions are shown in Figure 6. Controlled hammer impact tests were used to introduce particles into the ion beam path within the analyzer magnet region. High speed video cameras positioned at the entrance and exit of the second magnet verified the occurrence of particle “fire-fly’s” trapped within the beam entering the second magnet during this impact test, though no “fire-fly” particles were visible at the magnet exit. Figure 6 particle measurement results from the impact test show significant particle excursions levels at the pre-second magnet wafer position in comparison to negligible particle increase levels at the post-second magnet wafer position. Particle measurements collected with induced ion beam contact with the mass resolving slit (MRS) also show substantially elevated particle levels at the pre second magnet wafer position compared to zero particle levels at the post second magnet position. This type of beam strike condition simulates poorly optimized analysis AMU tuning, for instance.

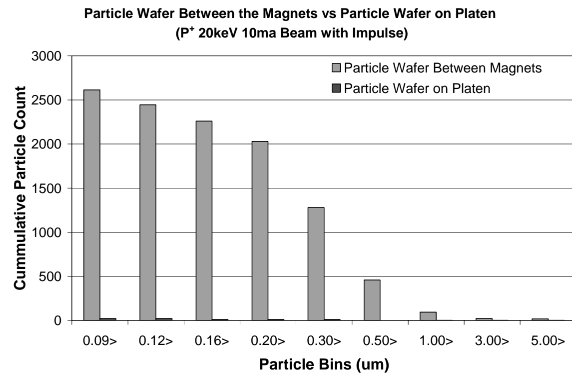

FIGURE 6. On-wafer particle data comparing a wafer placed between the magnets vs a wafer on the platen. An impulse was provided on the analyzer magnet to initiate beam-borne particles.

DISCUSSION

Reference [2] provides strong evidence that particles can be trapped electrostatically within an intense ion beam and transported down the beam-line by momentum transfer from the ions, even through bending magnets. This evidence appears at first to contradict the experimental data presented here. However, differences between the spot beam used by Sferlazzo et al and the nature of the ribbon beam examined here can modify the beam’s ability to trap particles. To extend this previous work [2] we have constructed a simple model to compare spot and ribbon beams. Consider the electric field in a beam with uniform charge density over an elliptical cross

section as shown in Figure 7. The uniform charge density required for dose uniformity in a ribbon beam tool makes this a reasonable approximation. While this is not necessarily true for a spot beam tool, the uniform charge density is consistent with minimizing the beam potential.

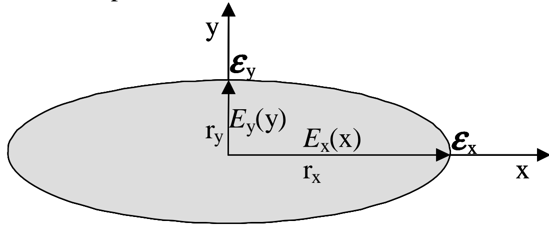

FIGURE 7. Elliptical cross section ion beam with uniform charge density and electric fields E_x and E_y.

A solution to Poisson's Equation requires that

$$E_x(x) = (\mathcal{E}_x/r_x)x, \quad E_y(y) = (\mathcal{E}_y/r_y)y$$

where $\mathcal{E}_x$ and $\mathcal{E}_y$ are the values of the field components at the boundary (i.e., at the points $x = r_x$ and $y = r_y$). Following Kellerman [3], $\mathcal{E}_x$ and $\mathcal{E}_y$ are determined by the charge density, $\rho = \frac{I}{Area}\sqrt{\frac{m}{2E}}$, and boundary conditions. For the case where the beam is surrounded by a conducting wall,

$$\frac{\mathcal{E}_x}{\mathcal{E}_y} = \frac{1}{k},$$

$$E_x = \frac{\rho}{\varepsilon_0}\frac{x\, r_y^2}{(r_x^2 + r_y^2)} \qquad E_y = \frac{\rho}{\varepsilon_0}\frac{y\, r_x^2}{(r_x^2 + r_y^2)}$$

The question is whether this field can provide sufficient force on a particle to cause it to curve along with the beam as the beam is bent by a magnetic field. The magnitude of this required centripetal force depends on the particle's diameter *d* and magnet radius *R*.

$$F_{cent} = \frac{\pi d^3 \delta v^2}{R},$$

where δ is the density of the particle, and *v* is the velocity of the particle due to momentum transfer from the beam ions (*v* typically ranges from ~10m/s – 50m/s [2]).

To find the electrostatic force on a particle, we need its charge in the beam plasma. This depends on the beam's electron temperature, and is difficult to calculate [2]. However, it is reasonable to assume that the particle will charge (negatively) such that its "floating" potential V_f will be within ~10V. From this assumption we can obtain a reasonable upper limit on the particle's charge Q , assuming it is spherical:

$$Q_{particle} = 2\pi\varepsilon_0 V_f d$$

As a figure of merit, we consider the following situation: A graphite particle of diameter .1µm is traveling within a 20kV P 10mA ribbon beam that is assumed to be 99% neutralized. The beam is then magnetically deflected horizontally with a radius of .6m. If the particle has attained a velocity of 10m/s, then the minimum electrostatic force needed from the space charge of the beam to transport the particle through the magnet is $1.75\text{x}10^{-16}$ N. If the beam's half width and height are r_x=15cm and r_y=2cm, the maximum horizontal electrostatic field at the edge of the beam is 1.2N/C, and since $Q_{particle}$~$5.6\text{x}10^{-17}$ C, the maximum beam confinement force is $6.5\text{x}10^{-17}$ N, which is less than the needed centripetal force to trap the particle. However, for a spot beam of diameter 6cm, the electrostatic confinement for the same conditions is $4.7\text{x}10^{-15}$ N, which more than an order of magnitude greater than the required confinement force.

SUMMARY

The Varian VIISta HC single wafer ion implanter architecture incorporates a dual magnet design. Demonstrated world-class particle level performance is the standard for this architecture. Experimental results show that this second magnet in conjunction with the ribbon beam optics properties serves as a critical particulate transport barrier. The derived model provides the basis for the particle performance of this architecture.

ACKNOWLEDGMENTS

We would like to thank Alex Perel, Joe Olson and Frank Sinclair for their contributions to this paper.

REFERENCES

1. L. Pipes, M. Taylor, G. Zietz, A. Al-Bayati, M Castle, T. Marin and J. Simmons, "Characterization and reduction of a new particle defect mode in sub-0.25um semiconductor process flows," *Proc. 15th Int. Conf. on Ion Implantation Tech.* (2004).
2. P. Sferlazzo, D.A. Brown, S.E. Beck and J.F. O'Hanlon, "Experimental Evidence of Beam Particulate Transport in Ion Implanters," *Proc. Conf. on Ion Implantation Tech.* (1993) p. 565.
3. P. Kellerman, "Advanced Modeling Techniques for Analysis of High Current Ribbon Beam Transport and Control," *Proc. 16th Int. Conf. on Ion Implantation Tech (2006)*